

Article

Simple and Acid-Free Hydrothermal Synthesis of Bioactive Glass 58SiO₂-33CaO-9P₂O₅ (wt%)

Ta Anh Tuan ¹, Elena V. Guseva ¹, Nguyen Anh Tien ², Ho Tan Dat ³ and Bui Xuan Vuong ^{4,*}

¹ Faculty of Chemical Technologies, Kazan National Research Technological University, 420015 Tatarstan, Russia; taanhtuan84pt@hpu2.edu.vn (T.A.T.); leylaha@mail.ru (E.V.G.)

² Faculty of Chemistry, Ho Chi Minh City University of Education, Ho Chi Minh City 700000, Vietnam; tienna@hcmue.edu.vn

³ Chu Van An Secondary School, Ho Chi Minh City 700000, Vietnam; tandatsphoahoc@gmail.com

⁴ Faculty of Pedagogy in Natural Sciences, Sai Gon University, Ho Chi Minh City 700000, Vietnam

* Correspondence: bxvuong@sgu.edu.vn

Abstract: The paper focuses on the acid-free hydrothermal process for the synthesis of bioactive glass. The new method avoids the use of harmful acid catalysts, which are usually used in the sol-gel process. On the other hand, the processing time was reduced compared with the sol-gel method. A well-known ternary bioactive glass 58SiO₂-33CaO-9P₂O₅ (wt%), which has been widely synthesized through the sol-gel method, was selected to apply to this new process. Thermal behavior, textural property, phase composition, morphology, and ionic exchange were investigated by thermal analysis, N₂ adsorption/desorption, XRD, FTIR, SEM, and inductively coupled plasma optical emission spectrometry (ICP-OES) analysis. The bioactivity and biocompatibility of synthetic bioactive glass were evaluated by in vitro experiments with a simulated body fluid (SBF) solution and cell culture medium. The obtained results confirmed that the acid-free hydrothermal process is one of the ideal methods for preparing ternary bioactive glass.

Keywords: bioactive glass; acid-free hydrothermal; bioactivity; hydroxyapatite; cell viability

Citation: Tuan, T.A.; Guseva, E.V.; Tien, N.A.; Dat, H.T.; Vuong, B.X. Simple and Acid-Free Hydrothermal Synthesis of Bioactive Glass 58SiO₂-33CaO-9P₂O₅ (wt%). *Crystals* **2021**, *11*, 283. <https://doi.org/10.3390/cryst11030283>

Received: 3 February 2021

Accepted: 8 March 2021

Published: 12 March 2021

Publisher's Note: MDPI stays neutral with regard to jurisdictional claims in published maps and institutional affiliations.



Copyright: © 2021 by the authors. Licensee MDPI, Basel, Switzerland. This article is an open access article distributed under the terms and conditions of the Creative Commons Attribution (CC BY) license (<http://creativecommons.org/licenses/by/4.0/>).

1. Introduction

Bioactive glasses (BGs) have been applied as bone fillers within the clinic for the past fifty years owing to their osteoconductivity and osteoinductivity [1]. These materials possess a special ability to attach to the bone tissue through the formation of a mineral hydroxyapatite layer when soaked in a biological solution. In this way, broken and defective bones are repaired and filled [2]. Since the primary discovery of bioactive glass (45SiO₂-24.5CaO-24.5Na₂O-6P₂O₅, wt%; the commercial name is Bioglass[®] or Novamin), many glass systems have been studied and synthesized using two main methods: melting and sol-gel [3,4]. In particular, the sol-gel method shows outstanding advantages compared to the melting method. The sol-gel processes are often applied to fabricate bioactive glasses at lower temperatures, preventing the loss of the ultimate product due to the evaporation of P₂O₅. Specifically, this method can synthesize bioactive glasses on a nano-scale with a high value of the specific surface area and porous structures, which improves the bioactivity of synthetic materials [5,6]. Nevertheless, most sol-gel processes have used harmful strong acids and bases as catalysts for the hydrolysis of precursors [7–17]. This affects the manufacturer's health when synthesizing the glass systems as well as the possibility of toxic acid residues in the final synthetic product. Therefore, finding acid-free synthesis methods can be seen as an urgent need to create friendly products that can be used as artificial bone materials or as additives in healthcare products. Recently, some scientists have reported on the synthesis of bioactive glasses by the green chemical process. Following this trend, new synthesis processes are being established to cut back or

eliminate the utilization or generation of harmful substances [18,19]. A quaternary bioactive glass 75%SiO₂-16%CaO-5%Na₂O-4%P₂O₅ (mol%) has been synthesized by the acid-free sol-gel process [20]. The authors rapidly added the precursors TEOS and TEP in an exceedingly large volume of water, under strong stirring of 1100 rpm. In this way, the alkoxides hydrolyzed completely to create a transparent sol after 5 h. In our previous studies, binary bioactive glasses 70Si-30Ca (mol%) with or without Zn doping, were made by the acid-free hydrothermal process [21,22]. The mixtures of suitable precursors without catalytic acids were heated in a Teflon-lined stainless steel autoclave at 150 °C in an electric oven and kept there for 1 day. The resulting product, in gel form, was dried and heat-treated at 700 °C for 3 h. The obtained glasses were amorphous materials and showed interesting bioactivities. For this paper, we applied the acid-free hydrothermal method to synthesize a well-known sol-gel bioactive glass 58SiO₂-33CaO-9P₂O₅ (wt%). Moreover, the advantage of the selected Na-free ternary system SiO₂-CaO-P₂O₅ avoids the negative effect of a sodium element. The release of sodium ions can cause a rapid pH increase, which can result in a cytotoxic effect [23–25]. By changing some conditions, like hot temperatures and the water/TEOS molar ratio, compared to previous studies [21,22], we emphasize that the acid-free hydrothermal process can be completely applied to synthesizing ternary bioactive glass 58SiO₂-33CaO-9P₂O₅ (wt%). The synthetic glass was characterized and examined for its bioactivity and biocompatibility.

2. Materials and Methods

2.1. Acid-Free Hydrothermal Synthesis

The acid-free hydrothermal process was used to prepare the bioactive glass 58SiO₂-33CaO-9P₂O₅ (wt%). The composition of the glass system was selected as in previous studies, where the material system was synthesized by the sol-gel method [14–17]. A brief description, a mixture containing 10.42 g of TEOS (tetraethyl orthosilicate, Sigma-Aldrich, ≥ 99.0%, Pcode: 102068011), 1.21 g of TEP (triethyl phosphate, Merck, 100%, CAS-No:78-40-0), 7.09 g of Ca(NO₃)₂·4H₂O (calcium nitrate tetrahydrate, Merck, 100%, CAS-No-13477-34-4), and 54 g of H₂O was stirred for 30 min. The H₂O/TEOS molar ratio was surveyed and selected at 60. After being mixed together, the mixture was placed in a stainless steel autoclave lined with a Teflon core. The hydrothermal synthesis reactor was programmed at 160 °C for 24 h. The gel-producing product was dried at 100 °C for 24 h to form the gel powder. From the thermal analysis data, the bioactive glass was obtained by sintering the dried powder at around 700 °C, with a heating rate of 10 °C/min, and kept there for 3 h.

2.2. In Vitro Experiment in SBF Fluid

An in vitro test is critical to confirm the bioactivity of synthetic biomaterials before in vivo tests in the animal body. The in vitro test was proposed by Kokubo and Takadama through the immersion of the material in the simulated body fluid (SBF) and widely applied for bioactivity evaluation [26]. The SBF synthetic solution had concentrations of inorganic ions almost similar to the blood of a human body (Table 1). It was synthesized by dissolving the appropriate chemical agents comprising MgCl₂·6H₂O, CaCl₂, K₂HPO₄·3H₂O, NaHCO₃, KCl, NaCl, and C₄H₁₁NO₃ in distilled water at a body temperature of 37 °C and a pH of 7.4. The powdered glasses were immersed in the SBF solution at 37 °C for 1, 3, and 5 days, with a stirring speed maintained at 60 rpm. At the end of each soaking stage, the powdered samples were refined, dried, and used for chemical–physical characterization. The remaining solutions were used for ionic measurements.

Table 1. Ionic concentration of the simulated body fluid (SBF) solution (mmol/L).

Composition	Na ⁺	K ⁺	Ca ²⁺	Mg ²⁺	Cl ⁻	HCO ₃ ⁻	HPO ₄ ²⁻
SBF	142.0	5.0	2.5	1.5	148.0	4.2	1.0
Plasma	142.0	5.0	2.5	1.5	103.0	27.0	1.0

2.3. In Vitro Assay Within the Cellular Medium

The cell culture medium was Dulbecco's Modified Eagle's Medium (DMEM; Merck, Product Code D9785) containing 10% fetal bovine serum (FBS), 100 $\mu\text{g mL}^{-1}$ of penicillin, 10 $\mu\text{g mL}^{-1}$ of streptomycin, and 15 mM of HEPES (4-(2-hydroxyethyl)-1-piperazineethanesulfonic acid). The L-929 fibroblast line was cultured in DMEM at a temperature of 37 °C in a humid incubator (5% CO₂, 95% humidity) for 24 h. The ratio of glass powder/medium was selected as 0.1 g mL⁻¹ according to the ISO standard 10993-12:2004. The various dilutions were obtained from the extract of the cellular medium, named as 20%, 40%, 60%, and 100% (without dilution). The fibroblast cells were exposed to the extracts for 24 h. The cellular viabilities on the bioactive glass were evaluated by the MTT (3-(4,5-Dimethylthiazol-2-yl)-2,5-Diphenyltetrazolium Bromide) method consistent with the previous study [27].

2.4. Characterization

The thermal behavior of the as-sintering bioactive glass was obtained by employing a Thermogravimetry–Differential Scanning Calorimetry (TG–DSC; Labsys Evo Setaram, Thermal Analysis Labs Ltd., Fredericton, NB, Canada). The fine glass powder was put in a platinum crucible and then heated up from 30 to 1000 °C at 10 °C/min in dried air. The textural properties were obtained by using N₂ adsorption/desorption on a micromeritics porosimeter (Quantachrome Instruments, Boynton Beach, FL, USA). The specific surface area was achieved by using the Brunauer–Emmett–Teller (BET) technique (Micrometrics, Georgia, USA). The pore size and pore volume were calculated from the isotherm desorption curve based on the Barrett–Joyner–Halanda (BJH) method. The phase characteristics of the powder samples were identified by X-ray diffraction (XRD; D8-Advance, Bruker, Billerica, MA, USA) with Cu-K α radiation ($\lambda = 1.5406 \text{ \AA}$). The measurements were performed within the range of 5–80° (2 θ), with a step of 0.02°. The XRD identification was performed by the X-Pert High Score Plus software. The chemical bonding groups were determined by a Fourier-Transform Infrared Spectroscopy (FTIR, Bruker Equinox 55, Bruker, Billerica, MA, USA). The spectral scan was carried out in the range of 400–4000 cm⁻¹, with a resolution of 2 cm⁻¹. Scanning Electron Microscopy (SEM) combined with Energy Dispersive X-ray Spectroscopy (EDX) (S-4800, Hitachi, Tokyo, Japan) was employed to identify the morphology and elemental composition of the powder samples. The ionic exchange in the SBF solution during the in vitro experiment was verified by using inductively coupled plasma optical emission spectrometry (ICP-OES, ICP 2060, Agilent, California, USA).

3. Results and Discussion

3.1. Thermal Behavior

The thermogravimetry (TG) and the differential scanning calorimetry (DSC) curves of the dried sample are presented in Figure 1. The TG curve shows three mass losses in the temperature ranges of 28–210, 210–405, and 405–670 °C. The primary mass loss corresponding to the endothermic peak at 129.4 °C on the DSC curve, is assigned to the physically adsorbed water removal [21,28]. The second one, with an exothermic peak at 298.2 °C on the DSC curve, is characteristic of the chemically adsorbed water release [29]. The last one, with an endothermic peak centered at 521.1 °C on the DSC branch, was due to the thermal decomposition of the NO₃⁻ groups used as oxide precursors [30,31]. An exothermic peak at 923.6 °C without the mass loss is attributed to the formation of wollastonite CaSiO₃ compound, according to our previous studies [21,22]. From temperatures above 670 °C, no mass loss was observed. Therefore, the suitable temperature for glass sintering is chosen to be at around 700 °C to eliminate the H₂O and NO₃⁻ components within the sample.

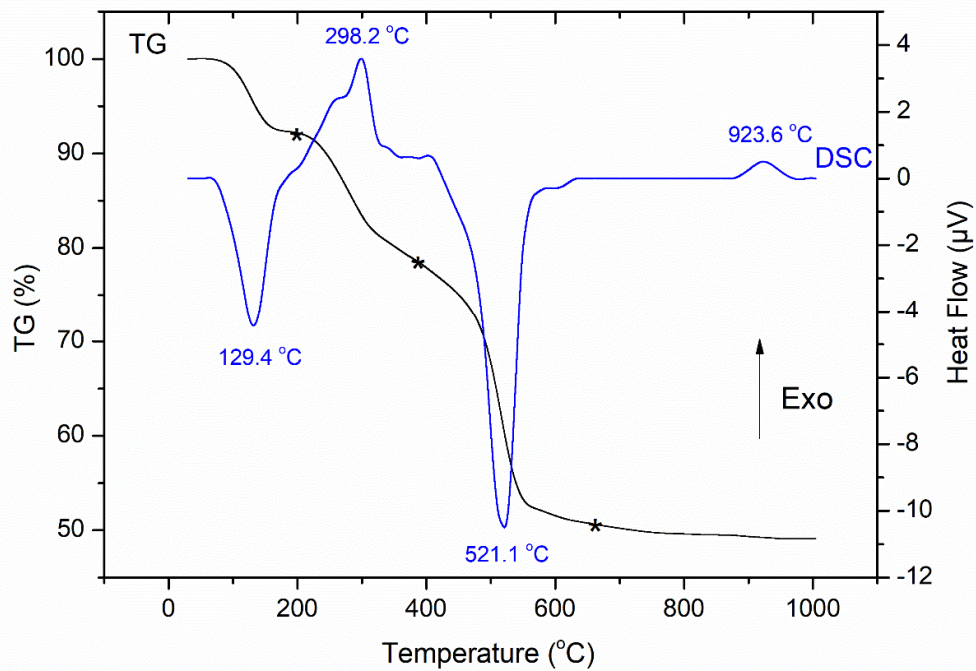


Figure 1. Thermogravimetry–Differential Scanning Calorimetry (TG–DSC) curves of the as-sintering bioactive glass sample.

3.2. Textural Analysis

The N₂ adsorption/desorption isotherm and pore size distribution of the bioactive glass powder are shown in Figure 2. The synthetic bioactive glass exhibited the type IV isotherm, which is suitable for mesoporous material based on the IUPAC classification of adsorption isotherms [32]. The BJH pore size distribution achieved from the desorption branch shows a relatively wide range and a single-type distribution with pore sizes of 8 to 90 nm, concentrated at a mean diameter (MD) of 21.2 nm. The measured values of the specific surface area (SSA) and pore volume (PV) are 104.7 m²/g and 0.54 cm³/g, respectively. In this study, the synthetic bioactive glass presents interesting values of SSA, PV, and MD compared to previous papers, as shown in Table 2 [15–17].

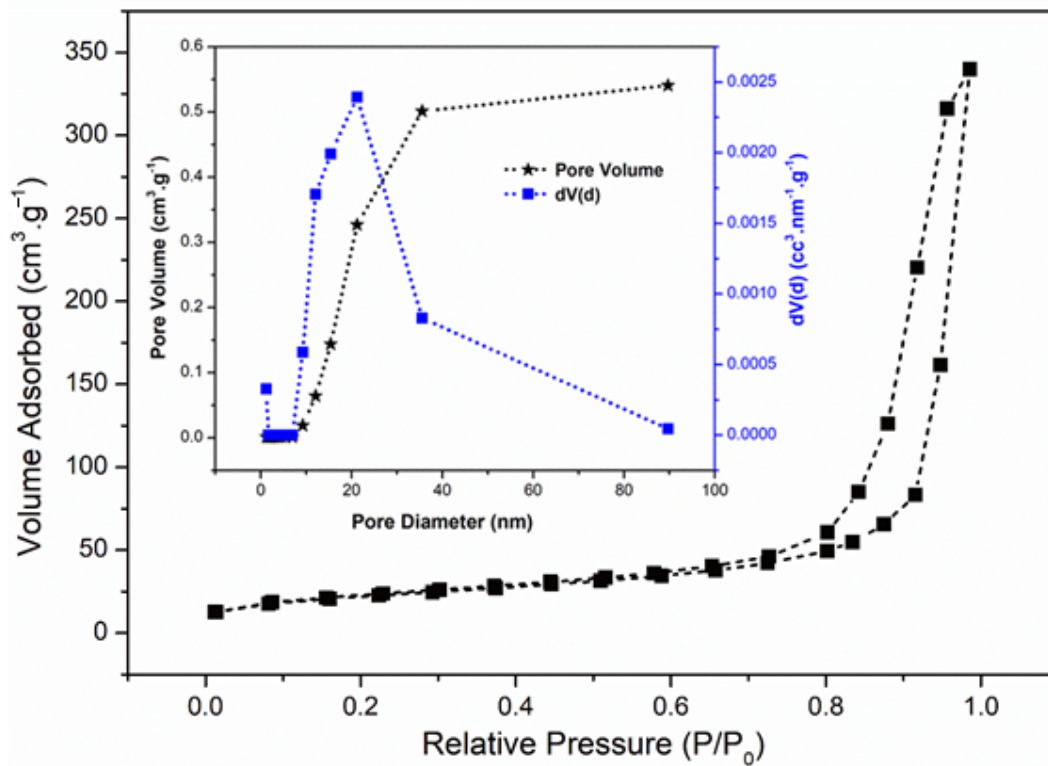


Figure 2. Nitrogen adsorption/desorption isotherm and pore size distribution of bioactive glass.

Table 2. Textural properties of synthetic bioactive glass.

Reference	Specific Surface Area (m ² /g)	Pore Volume (cm ³ /g)	Mean Diameter (nm)	Synthesis Method
[15]	82	0.201	10	Sol-Gel
[16]	99.1	-	-	Sol-Gel
[17]	126.54	0.447	6.55	Sol-Gel
[This Study]	104.7	0.54	21.2	Hydrothermal

3.3. Bioactivity Evaluation

3.3.1. XRD Analysis

Figure 3 shows the XRD diagrams of glass samples before and after the *in vitro* experiments in the SBF solution. The XRD pattern of the synthetic bioactive glass exhibits a wide diffraction halo centered at about 23° (2θ). This is a typical characteristic of an amorphous material, confirming the successful synthesis of ternary bioactive glass 58SiO₂-33CaO-9P₂O₅ (wt%) by the free-acid hydrothermal method. After the primary day in the SBF solution, the bioactive glass showed two well-defined peaks at 2θ = 26° (002) and 32° (211), which are attributed to the crystalline hydroxyapatite (HA) phase (well-matched with the JCPDS file no. 90432). As the soaking time increased, these two peaks became sharper and higher in intensity. After 5 days, most of the representative peaks of the HA phase appeared clearly, demonstrating the bioactivity of the synthetic bioactive glass in this study.

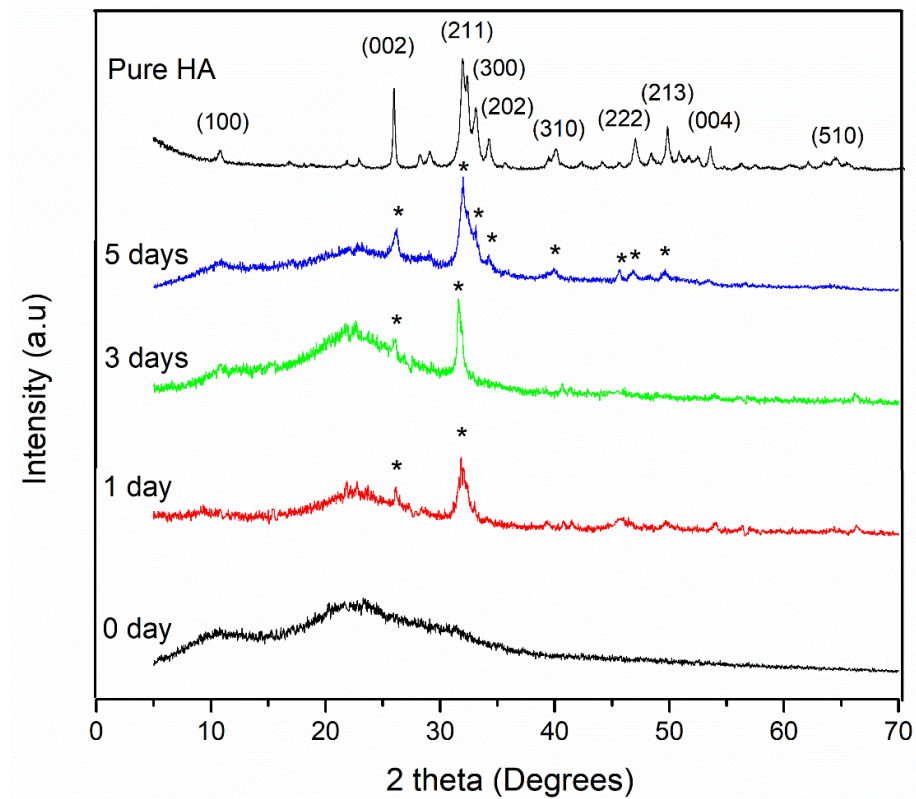


Figure 3. XRD diagrams of bioactive glass before and after the in vitro experiment in the SBF.

3.3.2. FTIR Analysis

Figure 4 represents the FTIR spectra of the bioactive glass before and after the in vitro experiment in the SBF. The spectrum of the synthetic glass represents the most characteristic bands of the silica network. The band at 1104 cm^{-1} is attributed to the Si-O-Si asymmetric stretching vibration (asym) while the band at 803 cm^{-1} corresponds to the Si-O-Si symmetric stretching vibration (sym) [33]. The band observed at 470 cm^{-1} is characteristic of the Si-O-Si bending vibration [34]. The weak band at 977 cm^{-1} is ascribed to the Si-O non-bridging oxygen (NBO) stretching mode [34]. Only a weak band at 554 cm^{-1} , related to the stretching mode of PO_4^{3-} [35,36], was observed because of the low content of P_2O_5 in the synthetic bioactive glass. After the in vitro experiment in the SBF for 1, 3, and 5 days, the spectral feature of the glass was modified, thanks to the chemical interactions between the glass samples and the physiological medium. The spectral band at 1104 cm^{-1} (Si-O-Si asym) was shifted to 1030 cm^{-1} . The band at 803 cm^{-1} (Si-O-Si sym) was moved to 869 cm^{-1} . The band at 470 cm^{-1} (Si-O-Si ben) was displaced to 460 cm^{-1} . The band at 977 cm^{-1} (Si-O-NBO) disappeared. The Si-O-Si shift and Si-O disappearance are associated with the glassy-network dissolution, and then the re-polymerization of the $-\text{Si}(\text{OH})_4$ groups to make the SiO_2 -rich surface layer [32–36]. Typically, two well-defined bands at 564 and 600 cm^{-1} are revealed. They are attributed to the stretching modes of the PO_4^{3-} groups in the hydroxyapatite crystals [37,38]. The FTIR results associated with the XRD analysis emphasize the bioactivity of bioactive glass synthesized by the free-acid hydrothermal method.

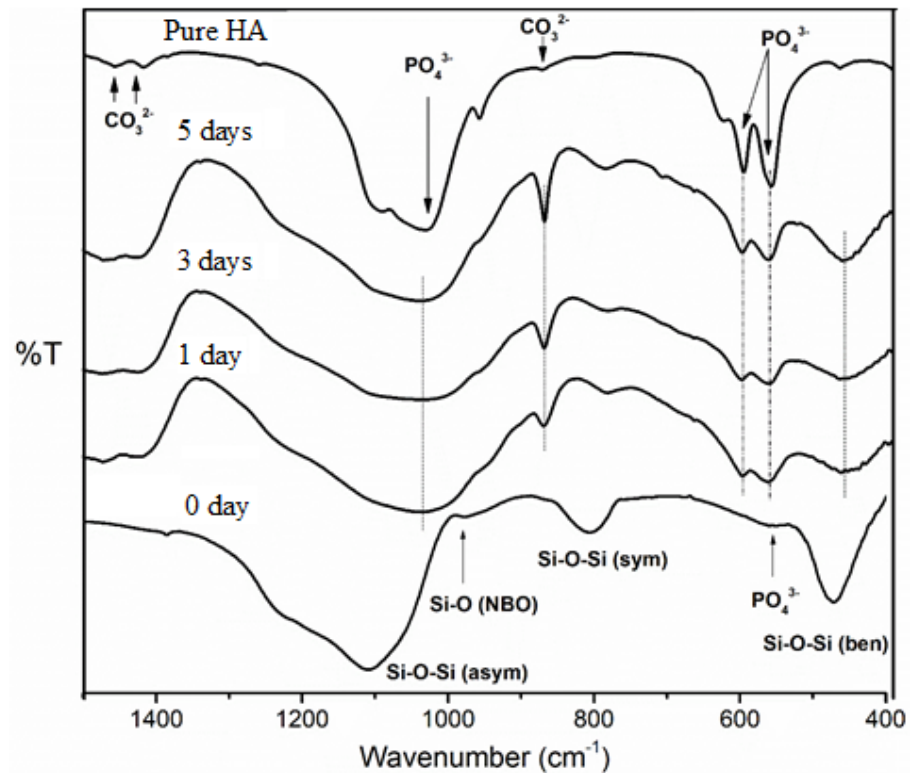


Figure 4. FTIR spectra of bioactive glass before and after the in vitro experiment in the SBF.

3.3.3. SEM–EDX Analysis

Figure 5 shows the SEM micrographs, including EDX analyses, of the glass samples before and after immersion in the SBF fluid for 5 days. The SEM image of the synthetic glass shows agglomerates consisting of intertwined tiny particles, forming the three-dimensional mesoporous structure of the synthetic material. The EDX analysis gives the Si/Ca/P molar ratio of 7.52:4.41:1, which is quite similar to the theoretical ratio in synthetic glass ($60\text{SiO}_2\text{-}36\text{CaO-}4\text{P}_2\text{O}_5$ mol%; Si/Ca/P = 7.5/4.5/1). After 5 days of immersion in the SBF solution, the surface of the bioactive glass was replaced and completely recovered by a uniform, scaled crystal layer. The EDX analysis of the glass after 5 days in SBF shows a decrease in Si content because of the degradation of the glassy network, and a rise in Ca and P amounts due to the formation of HA phase. The calculated Ca/P molar ratio for 5 days is 1.72, similar to that of pure apatite [30,31]. The SEM observation and EDX analysis confirmed the appearance of a new apatite layer on the surface of the bioactive glass.

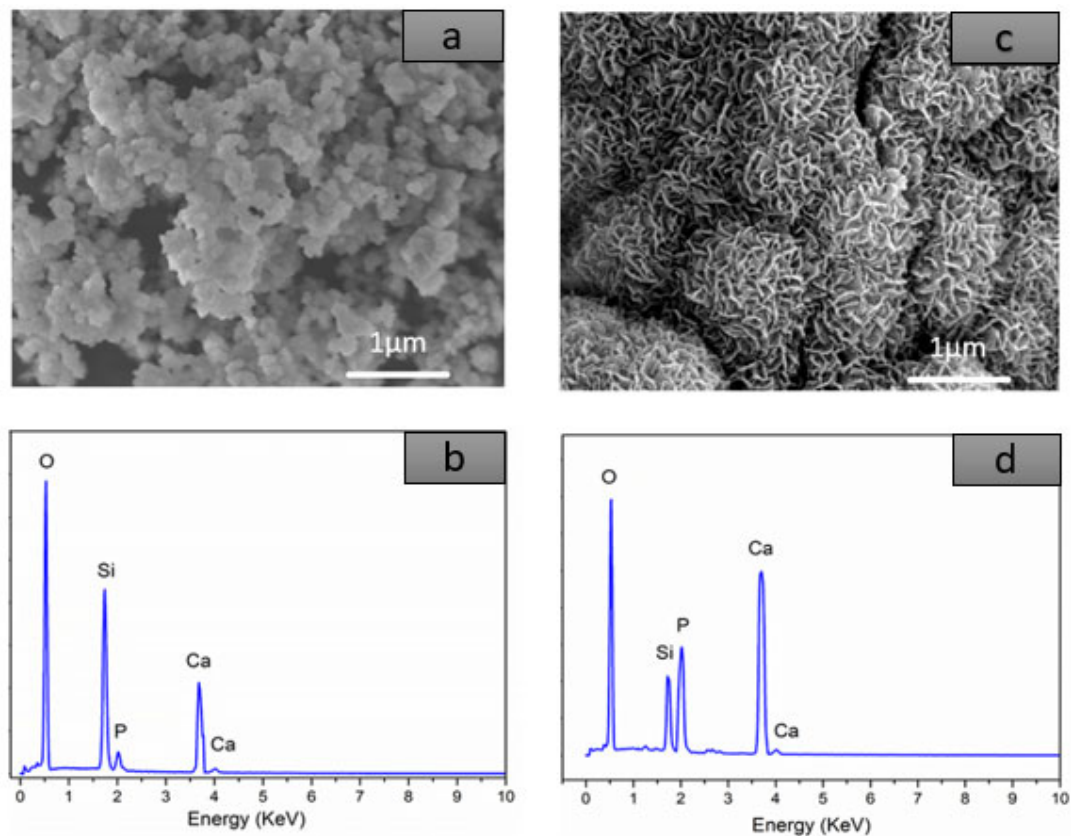


Figure 5. SEM–Energy Dispersive X-ray Spectroscopy (EDX) analyses of the bioactive glass: (a–b) before and (c–d) after 5 days of immersion.

3.3.4. ICP-OES Analysis

The physical–chemical interactions of the bioactive glass with the physiological environment led to ionic changes in the SBF solution as presented in the Figure 6. The elemental concentrations of Si, Ca, and P in the initial SBF solution were 0 ppm, 100.2 ppm, and 31.4 ppm, respectively. The Si concentration rapidly increased at the beginning time of soaking, and then moderately increased after 3 days. The concentration of Si reached the saturation value after 5 days of immersion. According to the previous studies, a rising in Si concentration is explained by the dissolution of the glassy network through the release of silicic acid $\text{Si}(\text{OH})_4$, while the saturation process corresponds to the re-polymerization of the above acids to create a SiO_2 silica layer [33–36]. On the other hand, the concentration of Ca increases at the beginning time of soaking, probably due to the quick exchange of Ca^{2+} out of the glassy network and H^+ in the physiological fluid [37–39]. Thereafter, the concentration of Ca strongly decreased after 3 days and reached saturation at 5 days. The decrease of the Ca concentration is expounded by its consumption to make the mineral HA layer on the surface of the bioactive glass [37–39]. By contrast, no increase in P concentration was observed after the *in vitro* experiment. This can be explained by the low content of P_2O_5 in the synthetic glass and also the rapid consumption of Ca and P for the formation of the apatite mineral layer. This result completely fits with the XRD analysis, where the HA layer was determined after just 1 day of soaking in the SBF solution.

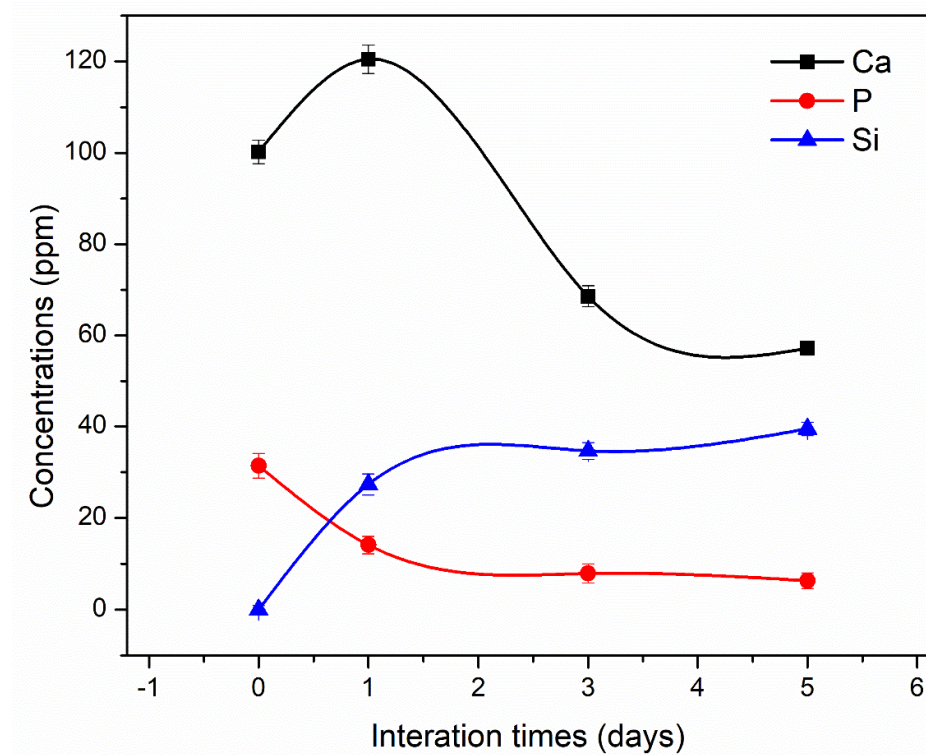


Figure 6. Ionic exchanges between the bioactive glass and the SBF solution.

3.4. Biocompatibility Evaluation

The cell viabilities of the L-929 fibroblast cells directly in contact with the bioactive glass powder for 24 h are presented in Figure 7. The cell viability without contact with the bioactive glass was selected as the control (100%) [27]. Following the standard ISO 10993-5 (Biological evaluation of medical devices – Part 5: Test for cytotoxicity, in vitro methods 2009), the cell viability was calculated as a percentage relative to the control, set as 100%. In the case where the average of cell viability was less than 70%, the material was cytotoxic. The obtained results show that the cell viabilities were 124, 116, 96, 94% for 20%, 40%, 60%, and 100% extracts, respectively. The 20% extract showed the highest value of cell viability, while the 60% and 100% extracts presented a small difference. Therefore, the bioactive glass $58\text{SiO}_2\text{-}33\text{CaO-}9\text{P}_2\text{O}_5$ (wt%) synthesized by the acid-free hydrothermal method presented good biocompatibility in the cellular medium even within the high extracts. The value of cell viability for the bioactive glass in this study is equivalent to those for previous glass systems, such as 45S5 melting Bioglass®, 77S sol-gel glass, and 58S sol-gel glass [40].

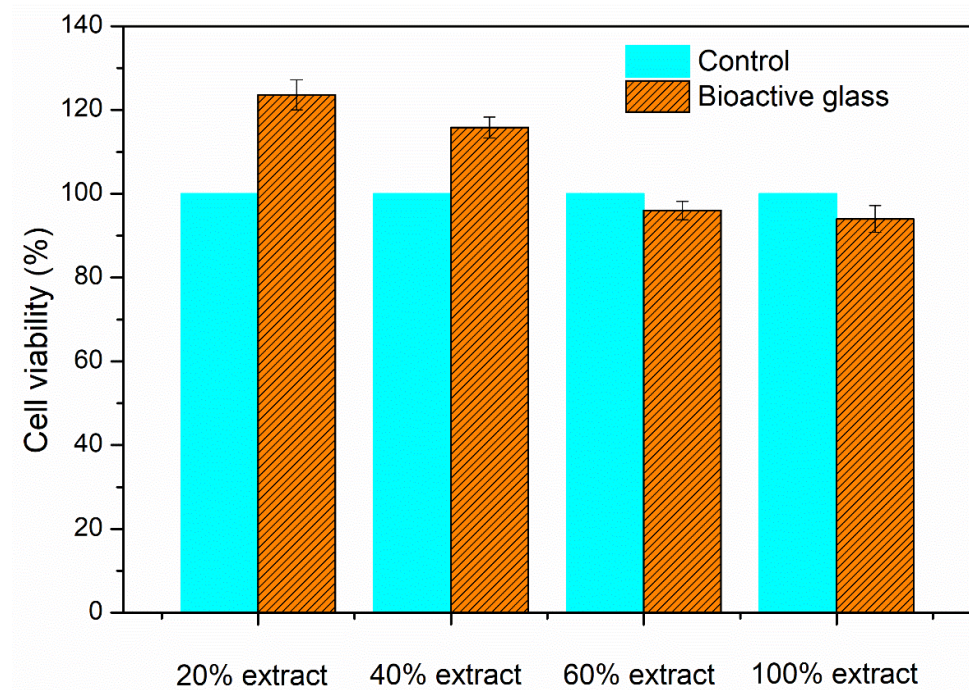


Figure 7. Cell viabilities of synthetic bioactive glass.

4. Conclusion

This study confirmed that the acid-free hydrothermal method is suitable for the synthesis of ternary bioactive glass $58\text{SiO}_2\text{-}33\text{CaO-}9\text{P}_2\text{O}_5$ (wt%). The obtained bioactive glass has amorphous and mesoporous structures. The bioactivity of the synthetic glass was proved through the rapid formation of the hydroxyapatite mineral layer on the surface of glass samples after an in vitro experiment in SBF. In addition, the in vitro experiment in the cellular environment demonstrated the good biocompatibility of the synthetic bioactive glass. The acid-free hydrothermal synthesis can be considered a new method to synthesize bioactive glass with properties similar to previous studies. The bioactive glass synthesized by this process, which does not use catalytic acids, can be used as artificial bone materials, and also can be used in food technology, such as additions to toothpaste or cosmetics.

Author Contributions: Tuan, T.A – Methodology, analysis, writing; Guseva, E.V – Writing, editing; Tien, N.A – Writing, editing; Dat, H.T – Methodology, analysis; Vuong, B.X – Writing, editing, analysis.

Funding: This research was funded by Sai Gon University, grant number TĐ 2020-2.

Institutional Review Board Statement: Not applicable.

Informed Consent Statement: Not applicable.

Data Availability Statement: Not applicable.

Conflicts of Interest: The authors declare no conflict of interest.

References

1. Rahaman, M.N.; Day, D.E.; Bal, B.S.; Fu, Q.; Jung, S.B.; Bonewald, L.F.; Tomsia, A.P. Bioactive glass in tissue engineering. *Acta Biomater.* **2011**, *7*, 2355–2373.
2. Hench, L.L. The story of Bioglass®. *J. Mater. Sci. Mater. Med.* **2006**, *17*, 967–978.
3. Julian, R.J. Review of bioactive glass: From Hench to hybrids. *Acta Biomater.* **2013**, *9*, 4457–4486.

4. Baino, F.; Novajra, G.; Pacheco, M.P.; Boccaccini, A.R.; Brovarone, C.V. Bioactive glasses: Special applications outside the skeletal system. *J. Non. Cryst. Solids*. **2016**, *432*, 15–30.
5. Boccaccini, A.R.; Erol, M.; Stark, W. Polymer/bioactive glass nanocomposites for biomedical applications: A review. *Compos. Sci. Technol.* **2010**, *70*, 1764–1776.
6. Zheng, K.; Boccaccini, A.R. Sol-gel processing of bioactive glass nanoparticles: A review. *Adv. Colloid Interface Sci.* **2017**, *249*, 363–373.
7. Sharifianjazi, F.; Parvin, N.; Tahriri, M.J. Synthesis and characteristics of sol-gel bioactive SiO₂-P₂O₅-CaO-Ag₂O glasses. *Non Cryst. Solids*. **2017**, *476*, 108–113.
8. Vulpoi, A.; Gruian, C.; Vanea, E.; Baia, L.; Simon, S.; Steinhoff, H.J.; Goller, G.; Simon, V. Silver effect on the structure of SiO₂-CaO-P₂O₅ ternary system. *Mater. Sci. Eng. C* **2012**, *32*, 178–183.
9. Balamurugan, A.; Balossier, G.; Kannan, S.; Michel, J.; Rebelo, A.H.S.; Ferreira, J.M.F. Development and in vitro characterization of sol-gel derived CaO-P₂O₅-SiO₂-ZnO bioglass. *Acta Biomater.* **2007**, *3*, 255–262.
10. Salman, S.; Salama, S.; Abo-Mosallam, H. The role of strontium and potassium on crystallization and bioactivity of Na₂O-CaO-P₂O₅-SiO₂ glasses. *Ceram. Int.* **2012**, *38*, 55–63.
11. El-Kheshen, A.A.; Khaliifaa, F.A.; Saad, E.A.; Elwana, R.L. Effect of Al₂O₃ addition on bioactivity, thermal and mechanical properties of some bioactive glasses. *Ceram. Int.* **2008**, *34*, 1667–1673.
12. Baino, F.; Fiume, E.; Miola, M.; Leone, F.; Onida, B.; Verné, E. Fe-doped bioactive glass-derived scaffolds produced by sol-gel foaming. *Mater. Lett.* **2019**, *235*, 207–211.
13. Bari, A.; Bloise, N.; Fiorilli, S.; Novajra, G.; Vallet-Regí, M.; Bruni, G.; Torres-Pardo, A.; González-Calbet, J.M.; Visai, L.; Vitale-Brovarone, C. Copper-containing mesoporous bioactive glass nanoparticles as multifunctional agent for bone regeneration. *Acta Biomater.* **2017**, *55*, 493–504.
14. Bini, M.; Grandi, S.; Capsoni, D.; Mustarelli, P.; Saino, E.; Visai, L.J. SiO₂-P₂O₅-CaO glasses and glass-ceramics with and without ZnO: Relationships among composition, microstructure, and bioactivity. *Phys. Chem. C* **2009**, *113*, 8821–8828.
15. Bejarano, J.; Caviedes, P.; Palzal, H. Sol-gel synthesis and in vitro bioactivity of copper and zinc-doped silicate bioactive glasses and glass-ceramics. *Biomed. Mater.* **2015**, *10*, 025001.
16. Bui, X.V.; Dang, T.H. Bioactive glass 58S prepared using an innovation sol-gel process. *Process. App. Ceram.* **2019**, *13*, 98–103.
17. Sepulveda, P.; Jones, J.R.; Hench, L.L. Characterization of melt-derived 45S5 and sol-gel-derived 58S bioactive glasses. *J. Biomed. Mater. Res.* **2001**, *58*, 734–740.
18. Sheldon, R.A.; Arends, I.W.C.E.; Hanefeld, U. *Green Chemistry and Catalysis*; Wiley VCH: Weinheim, Germany, 2007.
19. Clark, J.H.; Macquarrie, D.J. *Green Chemistry and Technology*; Abingdon: Nashville, TN, USA, 2008.
20. Ben-Arfa, B.A.E.; Fernandes, H.R.; Salvado, I.M.M.; Ferreira, J.M.F.; Pullar, R.C. Effects of catalysts on polymerization and microstructure of sol-gel derived bioglasses. *J. Am. Ceram. Soc.* **2018**, *101*, 2831–2839.
21. Hoa, B.T.; Hoa, H.T.T.; Tien, N.A.; Khang, N.H.D.; Guseva, E.V.; Tuan, T.A.; Vuong, B.X. Green synthesis of bioactive glass 70SiO₂-30CaO by hydrothermal method. *Mater. Lett.* **2020**, *274*, 128032.
22. Tuan, T.A.; Guseva, E.V.; Phuc, L.H.; Hien, N.Q.; Long, N.V.; Vuong, B.X. Acid-free Hydrothermal Process for Synthesis of Bioactive Glasses 70SiO₂-(30-x)CaO-xZnO (x = 1, 3, 5 mol.%). *Proceed.* **2020**, *62*, 1–12.
23. Fernandes, H.R.; Gaddam, A.; Rebelo, A.; Brazete, D.; Stan, G.E.; Ferreira, J.M.F. Bioactive glasses and glass-ceramics for healthcare applications in bone regeneration and tissue engineering. *Materials* **2018**, *11*, 2530.
24. Wallace, K.E.; Hill, R.G.; Pembroke, J.T.; Brown, C.J.; Hatton, P.V. Influence of sodium oxide content on bioactive glass properties. *J. Mater. Sci. Mater. Med.* **1999**, *10*, 697–701.
25. Kansal, I.; Reddy, A.; Muñoz, F.; Choi, S.; Kim, H.; Tulyaganov, D.U.; Ferreira, J.M.F. Structure, biodegradation behavior and cytotoxicity of alkali-containing alkaline-earth phosphosilicate glasses. *Mater. Sci. Eng. C* **2014**, *44*, 159–165.
26. Kokubo, T.; Takadama, H. How useful is SBF in predicting in vivo bone bioactivity? *Biomaterials* **2006**, *27*, 2907–2915.
27. Mosmann, T.J. Rapid colorimetric assay for cellular growth and survival: Application to proliferation and cytotoxicity assays. *Immunol. Meth.* **1983**, *65*, 55–63.
28. Saboori, A.; Rabiee, M.; Moztarzadeh, F.; Sheikhi, M.; Tahriri, M.; Karimi, M. Synthesis, characterization and in vitro bioactivity of sol-gel-derived SiO₂-CaO-P₂O₅-MgO bioglass. *Mater. Sci. Eng. C* **2009**, *29*, 335–340.
29. El-Kady, A.M.; Ali, A.F. Fabrication and characterization of ZnO modified bioactive glass nanoparticles. *Ceram. Int.* **2012**, *38*, 1195–1204.
30. Delben, J.R.J.; Pereira, K.; Oliveira, S.L.; Alencar, L.D.S.; Hernandez, A.C.; Delben, A.A.S.T. Bioactive glass prepared by sol-gel emulsion. *J. Non-Cryst. Solids*. **2013**, *361*, 119–123.
31. Román, J.; Padilla, S.; Vallet-Regí, M. Sol-gel glasses as precursors of bioactive glass ceramics. *Chem. Mater.* **2003**, *15*, 798–806.
32. Thommes, M.; Kaneko, K.; Neimark, A.V.; Olivier, J.P.; Rodriguez-Reinoso, F.; Rouquerol, J.; Sing, K.S.W. Physisorption of gases, with special reference to the evaluation of surface area and pore size distribution (IUPAC Technical Report). *Pure Appl. Chem.* **2015**, *87*, 1051–1069.
33. Aina, V.; Malavasi, G.; Pla, A.F.; Munaron, L.; Morterra, C. Zinc-containing bioactive glasses: Surface reactivity and behaviour towards endothelial cells. *Acta Biomater.* **2009**, *5*, 1211–1222.
34. Kim, I.Y.; Kawachi, G.; Kikuta, K.; Cho, S.B.; Kamitakahara, M.; Ohtsuki, C.J. Preparation of bioactive spherical particles in the CaO-SiO₂ system through sol-gel processing under coexistence of poly (ethylene glycol). *Eur. Ceram. Soc.* **2008**, *28*, 1595–1602.

35. Innocenzi, P.J. Infrared spectroscopy of sol–gel derived silica-based films: A spectra-microstructure overview. *Non-Cryst. Solids* **2003**, *316*, 309–319.
36. Ding, J.; Chen, Y.; Chen, W.; Hu, L.; Boulon, G. Effect of P₂O₅ addition on the structural and spectroscopic properties of sodium aluminosilicate glass. *Chin. Opt. Lett.* **2012**, *10*, 071602.
37. Chen, X.F.; Lei, B.; Wang, Y.J.; Zhao, N.J. Morphological control and in vitro bioactivity of nanoscale bioactive glasses. *Non-Cryst. Solids* **2009**, *355*, 791–796.
38. Hong, Z.; Liu, A.; Chen, L.; Chen, X.; Jing, X.J. Preparation of bioactive glass ceramic nanoparticles by combination of sol–gel and coprecipitation method. *Non-Cryst. Solids* **2009**, *355*, 368–372.
39. Hoppe, A.; Güldal, N.S.; Boccaccini, A.R. A review of the biological response to ionic dissolution products from bioactive glasses and glass-ceramics. *Biomaterials* **2011**, *32*, 2757–2774.
40. Silver, I.A.; Deas, J.; Hska, M.E. Interactions of bioactive glasses with osteoblasts in vitro: Effects of 45S5 Bioglass[®], and 58S and 77S bioactive glasses on metabolism, intracellular ion concentrations and cell viability. *Biomaterials* **2001**, *22*, 175–185.